Limits on Extra Dimensions and New Particle Production in the Photon and Missing Energy Signature in $p\bar{p}$ Collisions at $\sqrt{s} = 1.8$ TeV

A large group of people, P. Onyisi,[1] and H. Frisch[1]

(The CDF Collaboration)

[1] *University of Chicago*

(Dated: March 27, 2002)

The photon + $\not{E}_{\mathrm{T}}$ signal has a small standard model cross-section and is thus a good channel in which to look for signs of new physics. This signature is predicted by models with a superlight gravitino or with large extra dimensions. We search for such signals at the CDF detector at the Tevatron, using 87 pb^{-1} of data at $\sqrt{s} = 1.8$ TeV, and extract 95% C.L. limits on new processes. A limit of 221 GeV is set on the scale $|F|^{1/2}$ in supersymmetry models. For 4, 6, and 8 extra dimensions, limits on the fundamental mass scale, M_D, of 549, 581, and 602 GeV, respectively, are found. We also specify a 'pseudo-model-independent' method of comparing our results to theoretical predictions.

PACS numbers: 13.85.Rm, 14.80.-j

Many extensions to the standard model predict the existence of minimally-interacting particles, such as the gravitino in supersymmetric models and Kaluza-Klein modes of the graviton in models with large extra dimensions [1]. Such particles cannot be directly observed in a detector, but their production can be inferred from a transverse momentum imbalance, $\not{E}_{\mathrm{T}}$ [2], among the visible particles in a high-energy collision. Many models also predict the production of photons from the decay of final-state particles [3]; in addition photons may be emitted in any hard-scattering process due to the presence of charged quarks in the $p\bar{p}$ initial state. A search for the $\gamma\not{E}_{\mathrm{T}}$ signature thus explores a wide range of models and complements searches in the jet+$\not{E}_{\mathrm{T}}$ channel (see, for example, Ref. [4]).

The data used for this analysis were collected by the Collider Detector at Fermilab during Run 1b of the Tevatron, with an integrated luminosity of 87 $\pm$ 4 pb^{-1}. The CDF detector has been described in detail elsewhere [5]; subsystems most important to this search are summarized here. A system of time projection chambers around the beampipe allows the determination of the event vertex position. Surrounding these chambers, the central tracking chamber (CTC), a cylindrical drift chamber inside a 1.4 T superconducting solenoid, covers the pseudorapidity region $|\eta| < 1.1$ [6]. The central electromagnetic calorimeter (CEM) covers the region $|\eta| < 1.1$; strip chambers (the CES system) are embedded in the CEM and allow the measurement of the 2-dimensional transverse profile of an electromagnetic shower. The central hadronic calorimeters cover the range $|\eta| < 1.3$, and are instrumented with time-to-digital converters which associate times to shower signals. The calorimeter modules are arranged in a projective geometry pointing at the center of the detector; electromagnetic showers tend to be contained within a single module of the calorimeter, and high energy showers frequently leak from the electromagnetic calorimeters into the hadronic calorimeters behind them. When this leakage occurs, timing can be associated with the electromagnetic shower. Outside the calorimeters, drift chambers provide muon identification in the region $|\eta| < 1.0$.

To select events with high-p_{T} photons during data-taking, we use the CDF 3-level trigger system [7]. Level 1 requires a calorimeter tower with ${E_{\mathrm{T}}}^{EM} > 8$ GeV [6]. The level 2 system forms clusters of towers and then requires the event to pass an OR of several triggers, including: a) a very loose trigger requiring only an electromagnetic cluster[8] with ${E_{\mathrm{T}}}^{EM} > 50$ GeV, and b) a trigger requiring $\not{E}_{\mathrm{T}} > 35$ GeV. Level 3 requires that the photon candidate satisfy $E_{\mathrm{T}} > 50$ GeV and be within a fiducial region of the CEM.

The offline photon candidate identification criteria [9] further require: a) an electromagnetic cluster [10] in the CEM with $|\eta_\gamma| < 1$ [11] and a centroid within the fiducial region of the CES; b) shower evolution measured by the CES consistent with a nominal profile; c) no second energetic object nearby in the CES; d) at most one CTC track pointing at the cluster, with $p_{\mathrm{T}} \leq 1$ GeV/c; and e) E_{T} (excluding the photon cluster) < 2 GeV and a sum of track $p_{\mathrm{T}} < 5$ GeV/c within a radius of 0.4 in η-ϕ space around the cluster centroid.

To select the event topology, we require a) a primary vertex within 60 cm of the center of the detector; b) $E_{\mathrm{T}}^{\gamma} > 55$ GeV [12]; c) $\not{E}_{\mathrm{T}} > 45$ GeV; d) no jets with $E_{\mathrm{T}} > 15$ GeV; e) no jets with $E_{\mathrm{T}} > 8$ GeV within 0.5 radians in ϕ of the photon; and f) no tracks in the event with $p_{\mathrm{T}} > 5$ GeV/c.

Trigger and background considerations drive the

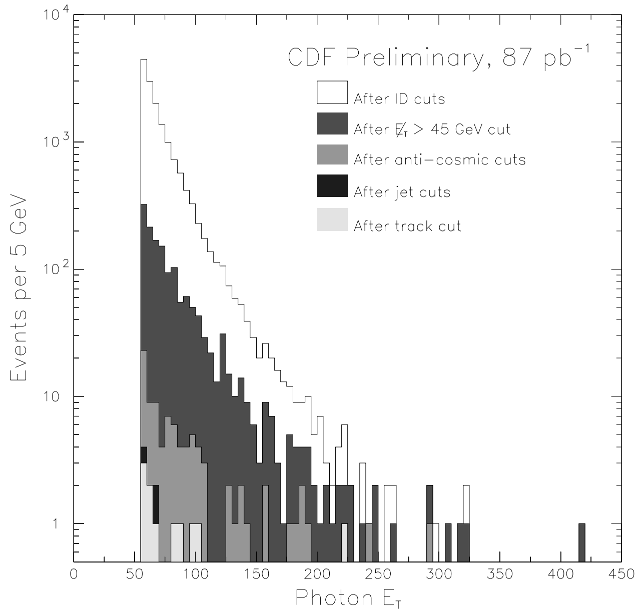

FIG. 1: E_T spectrum for events remaining after each stage of cuts

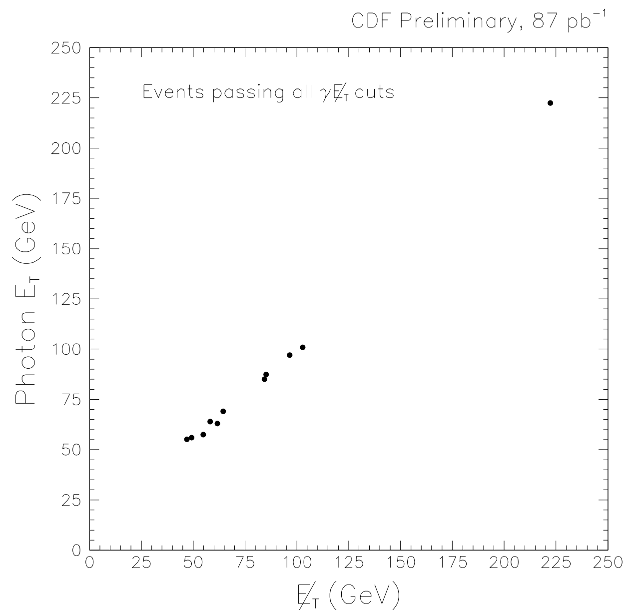

FIG. 2: Transverse energy versus missing transverse energy for events passing selection cuts

choice of the E_T^γ threshold. The level 3 trigger becomes fully efficient ($>$ 99%) at 55 GeV. In addition, below 45 GeV the background from $W \to e\nu$ with a misidentified electron (discussed further below) is very large; as the E_T^γ threshold is increased beyond the kinematic limit for electrons from W decay at rest, the W must recoil against another object, which is then rejected by the jet and track vetos.

To reduce the number of cosmic ray muons in the sample, we require a) a timing signal in the hadronic calorimeter for at least one tower in the cluster which is in-time with the collision within a 55 ns window; and b) no muon detections [13] in the central muon systems within 30° in ϕ of the photon.

The cumulative effects of each cut are shown in FIG. 1. The final sample after all cuts are applied contains 11 events, whose transverse energy and missing transverse energy are shown in FIG. 2.

The efficiency for the event topology cuts is dependent on the nature of the hard process. For a process producing only a photon and an invisible particle, with no jets, the overall efficiency for all cuts is found to vary from 0.45 at E_T = 55 GeV to 0.56 for $E_T >$ 100 GeV, with a 10% uncertainty.

Backgrounds to the photon + $\not\!\!E_T$ signal include: a) $q\bar{q} \to Z\gamma \to \nu\bar{\nu}\gamma$; b) cosmic ray muons that undergo bremsstrahlung in the CEM but for which we find no tracks; c) $W \to e\nu$, with the electron misidentified as a photon; d) $W\gamma$ production, where the charged lepton in a leptonic W decay is lost; e) prompt diphoton production, where a photon is lost; and f) other QCD processes. The expected number of events from each background source are indicated in Table I.

TABLE I: Background sources (note: numbers do not add due to rounding).

Cosmic rays	6.3 ± 2.0
$Z\gamma \to \nu\bar{\nu}\gamma$	3.2 ± 1.0
$W \to e\nu$	0.9 ± 0.1
Prompt diphotons	0.4 ± 0.1
$W\gamma$	0.3 ± 0.1
Total non-QCD background	11.0 ± 2.2
QCD background	0.9*
Total observed	11

* The uncertainty in this background is unknown, and this background is not considered when setting limits

To estimate the number of cosmic ray events in the signal sample, we use the events which have a timing signal *outside* the in-time window but which pass all other cuts. An extrapolation into the signal region, assuming a flat distribution in arrival time, gives 6.3 ± 2.0 events. This is the dominant background.

The Monte Carlo simulations of both backgrounds and signal processes use the PYTHIA event generator [14] with the CTEQ5L parton distribution functions [15], coupled with the CDF detector simulation package. We turn off initial state radiation (ISR) to obtain leading-order (LO) cross-sections and efficiencies. The resulting cross-sections are corrected by the ratio of the LO cross-section to the next-to-leading-order "0-jet" cross-section, obtained from known theoretical calculations and Monte Carlo estimates. This provides the correct estimate for the acceptance × efficiency × cross-section. The systematic uncertainties considered are Q^2 choice and acceptance variations due to modeling of the ISR. We estimate the γZ, γW and prompt diphoton backgrounds similarly with Monte Carlo simulations, obtaining correction factors of 0.95 ± 0.3 for $Z\gamma$ [16], 0.9 ± 0.2 for $W\gamma$ [17], and 1.0 ± 0.3 for prompt diphotons [18].

The background from $W \to e\nu$ arises either from hard bremsstrahlung by the electron before it enters the tracking chamber or inefficiency in the track reconstruction. As a radiated photon tends to be collinear with the electron, the $\mathrm{E_T}$ of the identified electromagnetic object will, in either case, be close to the initial energy of the electron. We assume a constant ratio $\mathcal{P}$ versus $\mathrm{E_T}$ between the number of electrons faking photons and the number of electrons passing electron cuts, and estimate $\mathcal{P}$ by assuming that "$e\gamma$" events with invariant masses within 10 GeV of the Z^0 mass are actually $Z^0 \to ee$ events. We find $\mathcal{P} = 0.8 \pm 0.1\%$. This probability is applied directly to a $W \to e\nu$ sample with the same jet and track vetos to obtain the background estimate.

We have investigated QCD backgrounds which involve detector mismeasurement of energy or misidentification of a jet as a photon. The apparent $\not\!\!E_{\mathrm{T}}$ in such events is due to jets falling into uninstrumented regions of the detector. A typical dijet or photon-jet event has two high-energy objects back-to-back in ϕ, with energies that approximately balance each other. Additional jets can appear due to fragmentation, gluon radiation, or jet reconstruction algorithm effects; for a given energy of the highest-energy ("leading") object the highest energies for the other objects will decrease with increasing multiplicity. The most likely contributors to fakes are thus events with one high-energy object and many low-energy jets. These events are rare and are very much on the tails of the $\not\!\!E_{\mathrm{T}}$, non-leading jet $\mathrm{E_T}$, and leading track $\mathrm{p_T}$ distributions. To estimate these backgrounds one must use data. However, the statistics are not sufficient to provide an estimate reliable to within an order of magnitude (estimates range from 0.1 to 2 events). We choose to take the conservative approach of not including this background source in the total background used in our limit calculations; this can only make the limits less stringent[19].

We study two hypothetical signal processes in detail. One is predicted by a supersymmetric model, and the other by a model with large compact extra dimensions.

The first process ($q\bar{q} \to \tilde{G}\tilde{G}\gamma$) is described in [20]. It presumes that the gravitino $\tilde{G}$ is the lightest supersymmetric particle, with the other superpartners too heavy to produce on-mass-shell at the Tevatron. Since the gravitino coupling is very small, being able to produce other supersymmetric particles increases the cross-section; we therefore set an absolute lower limit on the gravitino mass $m_{3/2}$ or, equivalently, the supersymmetry breaking scale $|F|^{1/2}$ (the two are related by $|F| = \sqrt{3}m_{3/2}M_P$, with M_P being the Planck mass). The cross-section for this process scales as $1/|F|^4$; there is no dependence on $|F|$ in the kinematic distributions.

The second process ($q\bar{q} \to \gamma G_{KK}$) is described in [21]: n extra spatial dimensions are assumed to be compactified with large radius R. The radius R and the fundamental mass scale M_D are related to Newton's constant and the number of extra dimensions by $G_N^{-1} = 8\pi R^n M_D^{2+n}$ [22]. The standard model fields propagate only on a 3+1 dimensional subspace, while gravitons propagate in the whole space. The graviton modes which propagate in the extra dimensions appear to four-dimensional observers as massive states of the graviton. A large value of R results in a large phase space for graviton production, canceling the weakness of the coupling to standard model fields. For a given n, the cross-section scales as $1/M_D^{n+2}$; there is no dependence on the parameter M_D in the kinematic distributions for fixed n.

The two signal processes are simulated with modified versions of PYTHIA. The $q\bar{q} \to \tilde{G}\tilde{G}\gamma$ process is simulated with $|F|^{1/2} = 100$ GeV, and the $q\bar{q} \to \gamma G_{KK}$ process is simulated with $M_D = 1$ TeV for $n = 4$, 6, and 8 extra dimensions.

We consider three sources of theoretical systematic uncertainty in the cross-section and acceptance predictions: uncertainty in the choice of Q^2 scale, the parton distribution function used, and the modeling of ISR. We obtain uncertainty estimates by varying Q^2 by a factor of 4 both up and down, by using the GRV 98 LO parton distribution functions [23], and by turning the modeling of ISR on and off. The uncertainty due to ISR includes order-α_s effects and acceptance changes due to the jet and track vetos. For $q\bar{q} \to \tilde{G}\tilde{G}\gamma$, the dominant uncertainty is the Q^2 choice ($^{+26}_{-18}\%$), followed by ISR ($\pm 14\%$) and PDF choice ($\pm 10\%$). For $q\bar{q} \to \gamma G_{KK}$, the dominant uncertainty comes from ISR ($\pm 34\%$), followed by Q^2 choice ($^{+18}_{-16}\%$) and PDF choice ($\pm 8\%$). The overall uncertainty in the $q\bar{q} \to \tilde{G}\tilde{G}\gamma$ acceptance × efficiency × cross-section, which includes a 10% uncertainty from efficiency corrections and detector modeling, is $^{+33}_{-27}\%$; for $q\bar{q} \to \gamma G_{KK}$, the corresponding figure

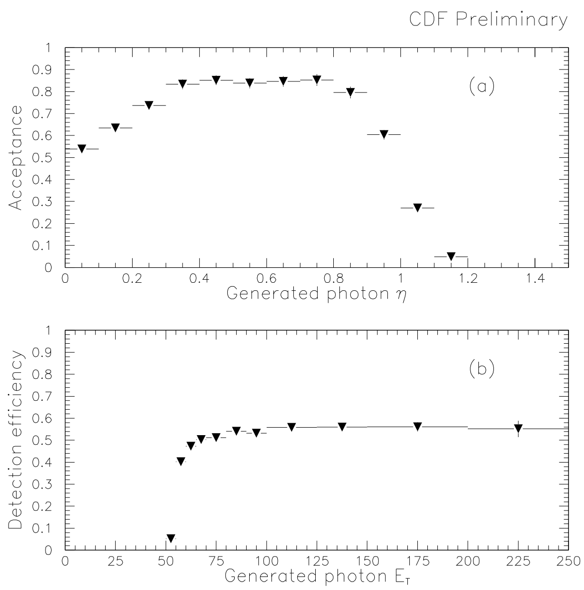

FIG. 3: Plots of (a) acceptance vs. photon η and (b) efficiency vs. photon $\mathrm{E_T}$ for processes that produce only a photon and an invisible particle.

is $^{+41}_{-40}\%$.

To set limits, we use a method derived from that of the Particle Data Group [24]. A 95% C.L. limit on a parameter α is defined as that value of α for which, in 95% of an ensemble of experiments, the number of events from background is less than the observed 11 and the total number of events from background and signal processes is greater than 11.

From this procedure, we find the following limits at 95% C.L.: for the supersymmetric model, $|F|^{1/2} \geq 221$ GeV (equivalently, $m_{3/2} \geq 1.17 \times 10^{-6}$ eV); for large extra dimensions, $M_D \geq 549$, 581, and 602 GeV for $n = 4$, 6, and 8 extra dimensions (equivalently, $R \leq$ 23.9 nm, 54.7 fm, and 2.61 fm, respectively) [25].

The results of this analysis can be presented in a 'pseudo-model-independent' manner. In both models that we have explicitly analyzed, the uncertainties in the predicted numbers of signal events have been dominated by theoretical factors. It can be useful to derive a cross-section limit which considers only the uncertainties in the detector simulation of the processes and so can easily be compared across models [26] (keeping in mind that such a limit is not a substitute for the rigorous extraction of a limit noting theoretical uncertainties). To obtain this limit, we compute a 95% C.L. upper limit on the number of events from new physics that would be detected, using the 10% detector uncertainty as the uncertainty in the cross-section for the new process. This limit is 9.8 events, which for this integrated luminosity corresponds to 112 fb.

The plots in FIG. 3 allow a comparison of a photon + invisible particle model to the data. By convolving the theoretical photon η and $\mathrm{E_T}$ spectra with the experimental acceptance and efficiency, one can obtain a good estimate of the acceptance × efficiency × cross-section for any LO photon + invisible particle signature.

We thank the Fermilab staff and the technical staffs of the participating institutions for their vital contributions. We would also like to thank J. Lykken, K. Matchev, and D. Rainwater for their help. This work was supported by the U.S. Department of Energy and National Science Foundation; the Italian Istituto Nazionale di Fisica Nucleare; the Ministry of Education, Science, Sports and Culture of Japan; the Natural Sciences and Engineering Research Council of Canada; the National Science Council of the Republic of China; the Swiss National Science Foundation; the A. P. Sloan Foundation; the Bundesministerium für Bildung und Forschung, Germany; and the Korea Science and Engineering Foundation.

[1] N. Arkani-Hamed, S. Dimopoulos, and G. Dvali, Phys. Lett. B **429**, 263 (1998).

[2] $\mathrm{E_T} \equiv \mathrm{E} \sin\theta$, where θ is the polar angle of the object measured relative to the event vertex. $\not{E}_{\mathrm{T}}$ is defined as the magnitude of the vector sum of $\mathrm{E_T}$ over all objects in the event.

[3] S. Ambrosanio, G. Kane, G. D. Kribs, S. P. Martin, and S. Mrenna, Phys. Rev. Lett. **76**, 3498 (1996).

[4] T. Affolder et al., Phys. Rev. Lett. **85**, 1378 (2000).

[5] F. Abe et al., Nucl. Instrum. Meth. Phys. Res., Sect. A **271**, 387 (1988).

[6] The CDF coordinate system is right-handed with the x axis horizontal and out of the Tevatron ring, the y axis up, and the z axis along the proton beam; ϕ is the azimuthal angle. The pseudorapidity $\eta \equiv -\ln(\tan(\theta/2))$, where θ is the polar angle; the η regions for detector components are defined with respect to the center of the detector.

[7] D. Amidei et al., Nucl. Instrum. Meth. **A350**, 73 (1994).

[8] The ratio of hadronic to electromagnetic energy is required to be less than 12.5%.

[9] See Refs. [26–28] for more details on photon identification in CDF.

[10] D. Amidei et al., Phys. Rev. D **50**, 2966 (1994).

[11] Here, η_γ is defined with respect to the center of the detector.

[12] The $\mathrm{E_T}$ and $\not{E}_{\mathrm{T}}$ values used in the offline selections are corrected values (see Ref. [10]).

[13] This is a 'stub' in the muon chambers; see Ref. [10] for more details.

[14] T. Sjöstrand et al., Computer Phys. Commun. **135**,

238 (2001), we use version 6.156.
[15] H. Lai et al., Phys. Rev. D **55**, 1280 (1997).
[16] U. Baur, T. Han, and J. Ohnemus, Phys. Rev. D **57**, 2823 (1998).
[17] U. Baur, T. Han, and J. Ohnemus, Phys. Rev. D **48**, 5140 (1993).
[18] B. Bailey, J. Ohnemus, and J. F. Owens, Phys. Rev. D **46**, 2018 (1992).
[19] Estimates of backgrounds with small central values but large uncertainties are necessarily highly asymmetric, as a background cannot be less than zero. During the limit-setting procedure, this would produce artificially high limits.
[20] A. Brignole, F. Feruglio, M. L. Mangano, and F. Zwirner, Nucl. Phys. B **536**, 136 (1998), erratum-ibid. **582**, 759 (2000).
[21] G. F. Giudice, R. Rattazzi, and J. D. Wells, Nucl. Phys. B **544**, 3 (1999), updated in hep-ph/9811291 v2.
[22] This is in the convention of Giudice et al.; other authors replace 8π by other values.
[23] M. Glück, E. Reya, and A. Vogt, Eur. Phys. J. C **5**, 461 (1998).
[24] R. Barnett et al., Phys. Rev. D **54**, 1 (1996).
[25] Unlike other limits set to date, these limits on M_D rise with n, because at the points at which we can set limits, the cross-sections rise with increasing numbers of extra dimensions.
[26] T. Affolder et al., hep-ex/0106012, to be published in Phys. Rev. D (2001).
[27] T. Affolder et al., Phys. Rev. D **59**, 092002 (1999).
[28] T. Affolder et al., hep-ex/0110015, submitted to Phys. Rev. D (2001).